Ionic Liquid–in–Oil Microemulsions Composed of Double Chain Surface Active Ionic Liquid as a Surfactant: Temperature Dependent Solvent and Rotational Relaxation Dynamics of Coumari...

ARTICLE *in* THE JOURNAL OF PHYSICAL CHEMISTRY B · JUNE 2012

Impact Factor: 3.3 · DOI: 10.1021/jp304668f · Source: PubMed

THE JOURNAL OF PHYSICAL CHEMISTRY B

Article

pubs.acs.org/JPCB

Ionic Liquid-in-Oil Microemulsions Composed of Double Chain Surface Active Ionic Liquid as a Surfactant: Temperature Dependent Solvent and Rotational Relaxation Dynamics of Coumarin-153 in [Py][TF_2N]/[C_4mim][AOT]/Benzene Microemulsions

Vishal Govind Rao, Sarthak Mandal, Surajit Ghosh, Chiranjib Banerjee, and Nilmoni Sarkar*

Department of Chemistry, Indian Institute of Technology, Kharagpur 721302, WB, India

Supporting Information

ABSTRACT: In the recent past, nonaqueous microemulsions containing ionic liquids (ILs) have been utilized for performing chemical reactions, preparation of nanomaterials, and synthesis of nanostructured polymers and in drug delivery systems. The most promising fact about IL-in-oil microemulsions is their high thermal stability compared to that of aqueous microemulsions. In our earlier publication (Rao, V. G.; Ghosh, S.; Ghatak, C.; Mandal, S.; Brahmachari, U.; Sarkar, N. *J. Phys. Chem. B* **2012**, *116*, 2850−2855), we presented for the first time the possibility of creating huge number of IL-in-oil microemulsions, just by replacing the inorganic cation, Na^+, of NaAOT by any organic cation and using different ionic liquids as the polar core. In this manuscript we are interested in exploring the effect of temperature on such systems. We have characterized the phase diagram of the [Py][TF_2N]/[C_4mim][AOT]/benzene ternary system at 298 K. We have shown that in the experimental temperature range employed in this study, the microemulsions remain stable and a slight decrease in the size of the microemulsions is observed with increasing temperature. We have reported the detailed study of solvent and rotational relaxation of coumarin 153 (C-153) in neat IL, *N*-methyl-*N*-propylpyrrolidinium bis((trifluoromethyl)sulfonyl)imide ([Py][TF_2N]), and in [Py][TF_2N]/[C_4mim][AOT]/benzene microemulsions using steady state and picosecond time-resolved spectroscopy. We have monitored the effect of (i) varying the [Py][TF_2N]/[C_4mim][AOT] molar ratio (*R* value) and (ii) temperature on solvent and rotational relaxation of C-153. The features observed in absorption and emission spectra clearly indicate that (i) the probe molecules reside at the polar interfacial region of the [Py][TF_2N]/[C_4mim][AOT]/benzene microemulsions and (ii) with increasing *R* value the probe molecules move toward the polar IL-pool of the microemulsion. We have shown that the increase in solvation time on going from neat [Py][TF_2N] to [Py][TF_2N]-containing microemulsions is very small compared to the increase in solvation time on going from pure water to water-containing microemulsions. The average solvation time decreases with increasing *R* values at 298 K, but it shows only a small *R* dependence compared to microemulsions containing solvents capable of forming hydrogen bonds. We have also shown that the temperature has substantial effect on the solvent and rotational relaxation of C-153 in neat [Py][TF_2N] compared to that of [Py][TF_2N]/[C_4mim][AOT]/benzene microemulsions at $R = 0.69$.

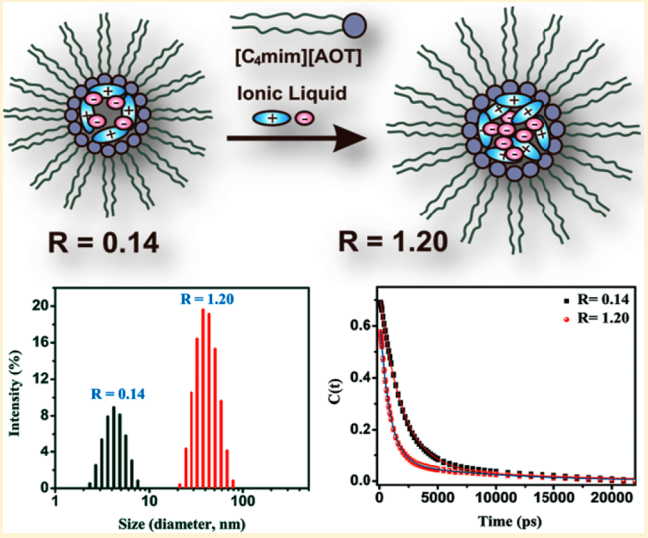

1. INTRODUCTION

Microemulsions are microheterogeneous systems consisting of two immiscible liquids (polar and nonpolar) and an amphiphilic component (usually surfactants and cosurfactants). They are capable of solubilizing both polar and nonpolar substances and have found wide applications[1−3] in various fields such as chemical reactions,[4,5] preparation of nanomaterials[6] and in drug delivery systems.[7] Traditionally microemulsions were formulated using water as the polar core and these systems have been extensively studied in the past.[8−15] However, in recent years several reports on nonaqueous microemulsions have appeared in the literature.[16−24] Chemical reactions that require a water-free environment,[25] such as Diels−Alder reaction, esterification, and polymerization,[26] can be successfully carried out in nonaqueous microemulsions. Besides the wide variety of conventional polar organic solvents[27] (e.g., ethylene glycol, formamide, glycerol etc.) that

Received: May 14, 2012
Revised: June 20, 2012
Published: June 21, 2012

can be used to replace water as the polar core of nonaqueous microemulsions, ionic liquids (ILs) are also a viable possibility.

ILs are low melting organic salts that are often associated with "green chemistry" because they possess certain advantageous properties typically linked to environment friendly solvents like negligible vapor pressure, wide electrochemical window, nonflammability, high thermal stability, and wide liquid range.[28] They are often designated as "designer solvents" because prudent combination of the constituent ions and suitable functionalization of the same allows one to gain control over the physical properties of an IL. Nowadays people are trying to replace simple salts and polar solvents like water by ionic liquids for the modification of physicochemical properties of different micellar aggregates.[16,17,19−21,29−33] In particular, the research into IL-containing nonaqueous microemulsions was motivated by the fact that in spite of the useful properties of ILs, poor solubility of apolar solutes in neat ILs was a major hindrance in the path of their potential application. This could be overcome using the hydrocarbon domains provided by IL-in-oil microemulsions.[34] The expected thermal stability of such a system over aqueous microemulsions was another appealing factor. Gao et al.[16] first reported the formation of IL-in-oil microemulsions in $[C_4mim][BF_4]$/TX-100/cyclohexane system. The size and shape of these microemulsions were verified from SANS studies by Eastoe et al.[17] where regular swelling behavior with the addition of the IL was also observed, which indicated that the volume of dispersed nanodomains was proportional to the amount of IL added. Following this, several other reports on similar systems appeared in the literature.[19−21,35]

Perhaps the most encouraging fact about IL-in-oil microemulsions is their potential for applications, a part of which is already being exploited, e.g., in the field of performing chemical reactions,[36,37] in the synthesis of nanostructured polymers,[38,39] and as drug delivery carrier.[40] One aspect of IL-in-oil microemulsions that we are currently interested in exploring is the effect of temperature on such systems. Gao et al.[41] investigated the effect of temperature on the microstructure of the two IL-in-oil microemulsions $[C_4mim][BF_4]$/TX-100/oil (cyclohexane and toluene). In contrast to aqueous microemulsions, these systems exhibited high temperature-independence. This difference in behavior was rationalized by considering the underlying stabilizing interactions that enables the formation of both types of microemulsions. Although aqueous microemulsions are stabilized by hydrogen bonding (HB) between the water molecules and the ethylene oxide (EO) moieties on the nonionic surfactant TX-100, electrostatic interaction between the $[C_4mim]^+$ ion and the EO groups drives the formation of their nonaqueous counterparts. The relative temperature insensitivity of the latter compared to the former is the cause of the observed thermal stability. Furthermore, Zech et al. stated that for formulation of microemulsions with high temperature stability and temperature insensitivity, it was better to use ionic surfactants in combination with ILs.[42] After observing the surfactant-like behavior of the surface active ionic liquid (SAIL) 1-hexadecyl-3-methylimidazolium chloride, $[C_{16}mim][Cl]$ in EAN, Zech et al. studied microemulsions of the type RTIL($[C_4mim][BF_4]$ and EAN)/$[C_{16}mim][Cl]$/dodecane using conductivity, DLS and SAXS measurements.[43] SAILs can be defined as functional ionic liquids with combined properties of ILs and surfactants, in other words ILs bearing long alkyl chains having amphiphilic character are named as surface active ionic liquids SAILs.[44,45] They explored the thermal stability of EAN-in-dodecane microemulsions using conductivity and SANS experiments.[42] The system chosen was EAN/$[C_{16}mim][Cl]$/dodecane and under ambient pressure, it exhibited stability over the temperature range 30 to 150 °C. Such microemulsions possess the potential for finding application in lubricant formulations or as reaction media.

The investigation of solvation dynamics can provide useful information regarding these microemulsions. Over the last three decades considerable efforts have been made to understand solvation dynamics in different heterogeneous media such as micelles, reverse micelles, microemulsions, lipids, proteins, DNA, etc.[46−56] Nowadays the solvation dynamics study of a newly created ion or a dipole in polar liquids is frequently utilized for obtaining molecular level information about the response of solvent molecules (which composed of both orientational and translational motions) to the probe.[46−48,57−59]

The interesting point for which we must pay our attention is that the solvation dynamics in RTILs are immensely different from that in the isopolar conventional solvents such as methanol, acetonitrile, and so on.[60−66] Solvation in RTILs takes place because of the diffusional motion of the constituents ions of ionic liquids around an excited dye, whereas in polar solvents like water, methanol, and acetonitrile, the solvation occurs as a result of as the reorientation of the solvent molecules. Recent ultrafast studies suggest that the difference is less striking than originally thought.[67,68] Chapman and Maroncelli[69] showed that solvation is guided by the viscosity of the solvents; ionic solvation is slower compared to the pure solvent. Bart et al.[70,71] showed that ionic solvation is slow and biphasic in nature. Samanta et al.[72−74] asserted that the fast component is due to the anions whereas the slow component results from a large-scale rearrangement of the ions around the photoexcited system. Petrich and co-workers observed that the polarizability of the cation is responsible for the fast component[75] and this was further supported by Song using Debye−Huckel dielectric continuum model.[76] Halder et al.[77] suggested that translational motion of ions may not be the predominant factor in the short time solvation of ionic fluids. According to Maroncelli et al.[78−80] the translation adjustment of the ions within the solvation structure present at the time of solute excitation is responsible for the observed fast component. Although Shim et al. have shown that the short component is due to the translational motion of the anions,[81,82] Kobrak and Znamenskiy have demonstrated that collective cation−anion motion is responsible for the fast component.[83] Simulation studies also suggest that solvation dynamics in RTIL involves collective motion of cations and anions.[84−87] According to present theory of Kashyap and Biswas,[88] the fast component of the solvation response function originates from the rapid orientational relaxation involving the dipolar species, whereas the relaxation of the ion dynamic structure factor via ion translation produces the observed slow nonexponential component.

Keeping in mind the facts mentioned regarding the high temperature stability of microemulsions, we have designed our system *N*-methyl-*N*-propylpyrrolidinium bis((trifluoromethyl)-sulfonyl)imide ($[Py][TF_2N]$)/$[C_4mim][AOT]$/benzene, such that the main stabilizing interaction (responsible for microemulsion formation) between the negatively charged AOT^- group of the surfactant and the RTIL which acts as the polar core is primarily electrostatic in nature. In our earlier

dx.doi.org/10.1021/jp304668f | J. Phys. Chem. B 2012, 116, 8210−8221

manuscript we have reported a technique for creating huge number of IL-in-oil microemulsions. It involved the use of an AOT-derived SAIL (which was synthesized by replacing the inorganic cation, Na^+, of NaAOT by an organic cation, $[C_4mim]^+$) alongside different ionic liquids as the polar core.[89] In the present case, we investigate the effect of temperature on such systems. For this we have utilized dynamic light scattering (DLS) measurements to show the size variation with temperature. We have utilized steady state and picosecond time-resolved spectroscopy to investigate the solvent and rotational relaxation of coumarin 153 (C-153) in neat $[Py][TF_2N]$ and in $[Py][TF_2N]/[C_4mim][AOT]$/benzene microemulsions. Finally, we have investigated and compared the effect of temperature on solvent and rotational relaxation of C-153 in neat $[Py][TF_2N]$ and in $[Py][TF_2N]/[C_4mim]$-$[AOT]$/benzene microemulsions.

2. EXPERIMENTAL SECTION

2.1. Materials. Coumarin-153 (C-153) (laser grade, Exciton) and benzene (Spectrochem, HPLC grade) were used as received. NaAOT (sodium 1,4-bis(2-ethylhexyl)-sulfosuccinate, Sigma-Aldrich) was dried in vacuum for 30 h before use. $[C_4mim][AOT]$ (synthesis reported in our earlier manuscript[89]) was dried in vacuum for 50 h at 60−70 °C before use. The RTIL, *N*-methyl-*N*-propylpyrrolidinium bis-((trifluoromethyl)sulfonyl)imide, $[Py][TF_2N]$ was obtained from Kanto chemicals (98% purity) and dried in vacuum for 24 h at 70−80 °C before use. The structure of $[C_4mim][AOT]$, $[Py][TF_2N]$, and Coumarin-153 are shown in Scheme 1.

2.2. Instrumentation. For the collection of steady state absorption and emission spectra we have used a Shimadzu (model number, UV-2450) spectrophotometer and a Hitachi (model number, F-7000) spectrofluorometer, respectively. All the samples were excited at 408 nm to collect the emission spectra. For time-resolved fluorescence measurements we have used a time-correlated single-photon-counting (TCSPC) instrument from IBH (U.K.). The instrument response function of our setup is ∼90 ps. The detailed time-resolved fluorescence setup is described in our earlier publication.[90,91] Briefly, the samples were excited at 408 nm using a picosecond laser diode (IBH, Nanoled), and the signals were collected at the magic angle (54.7°) using a Hamamatsu microchannel plate photomultiplier tube (3809U). The same setup was used for the anisotropy decay measurements in which we employed a motorized polarizer on the emission side. The emission intensities at parallel $I_{\parallel}(t)$ and perpendicular $I_{\perp}(t)$ polarizations were collected alternatively until a certain peak difference between parallel $I_{\parallel}(t)$ and perpendicular $I_{\perp}(t)$ decay was reached. The analysis of the fluorescence decay and anisotropy decay data were performed using IBH DAS, version 6 decay analysis software. For viscosity measurements, we used a Brookfield DV-II+ Pro (viscometer). The temperature was maintained by circulating water through the cell holder using a JEIO TECH Thermostat (RW-0525GS).

For DLS measurements, we used a Malvern Nano ZS instrument employing a 4 mW He−Ne laser (λ = 632.8 nm). In the data collection processes the scattering photons were collected at 173° scattering angle. The scattering intensity data were processed using the instrumental software to obtain the hydrodynamic diameter (d_h) and size distribution of the scattered data in each sample. The instrument measures the fluctuation in scattering intensity and uses this to calculate the size of particles within the sample. The d_h of the microemulsions were estimated from the intensity autocorrelation function of the time-dependent fluctuation in intensity. The d_h is defined as follows

$$d_h = \frac{k_B T}{3\pi\eta D} \quad (1)$$

where k_B is the Boltzmann constant, η is the viscosity, and D is the translational diffusion coefficient.

Scheme 1. Structures of Surface Active Ionic Liquid (SAIL), $[C_4mim][AOT]$, RTIL, $[Py][TF_2N]$ and Coumarin-153

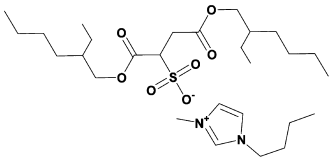

$[C_4mim][AOT]$

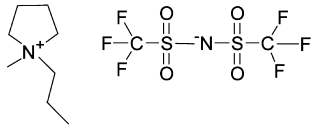

N-Methyl-N-propylpyrrolidinium bis (trifluoromethanesulfonyl) imide $[Py][TF_2N]$

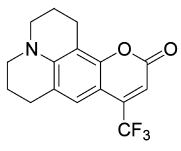

Coumarin-153

3. RESULTS AND DISCUSSION

3.1. Phase Behavior Study. Phase behavior study is one of the essential steps in characterization of microemulsions. We have characterized the partial phase diagram of the ternary system $[Py][TF_2N]/[C_4mim][AOT]$/benzene at 298 K by observing the transition from clear transparent solution to turbid solution visually, i.e., through the naked eye (Figure 1). Figure 1 clearly indicates that a continuous stable single phase microemulsion region can always be observed over the $[Py][TF_2N]$ or benzene content range of 0−100 wt %. On the basis of the phase diagram, a series of samples were chosen where we can have the possibility of IL/O microemulsions only (blue points). Interestingly, on comparing the phase behavior of $[Py][TF_2N]/[C_4mim][AOT]$/benzene ternary system with our earlier characterized $[Py][TF_2N]$/TX-100/benzene ternary system,[92] we found that the area of single phase region decreases on going from ionic SAIL ($[C_4mim][AOT]$) to nonionic TX-100. This large single phase region can be accounted for by the presence of similar nature of both the IL and SAIL in case of $[Py][TF_2N]$/TX-100/benzene ternary system.

3.2. Dynamic Light Scattering Measurements. In our earlier manuscript,[89] we have already established the formation of $[Py][TF_2N]/[C_4mim][AOT]$/benzene microemulsions. The size distribution and variation of size with increasing R

dx.doi.org/10.1021/jp304668f | J. Phys. Chem. B 2012, 116, 8210−8221

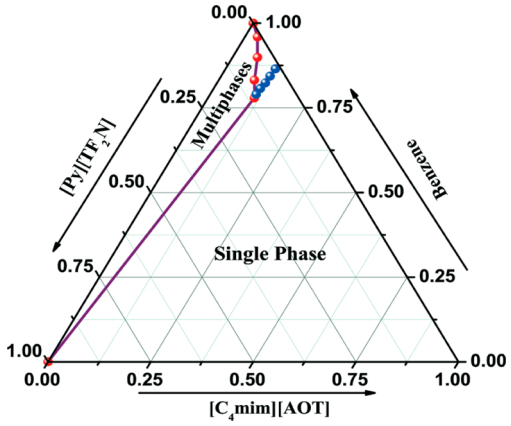

Figure 1. Phase diagram of the [Py][TF_2N]/[C_4mim][AOT]/benzene ternary system at 298 K. Blue points indicate the five different *R* values.

value reported there revealed a linear relationship between size and *R* up to *R* = 1.0, beyond which deviation from linearity was observed. Here we have investigated the effect of temperature on the size of the [Py][TF_2N]/[C_4mim][AOT]/benzene microemulsions at *R* = 0.69 (Figure 2). It is evident from the

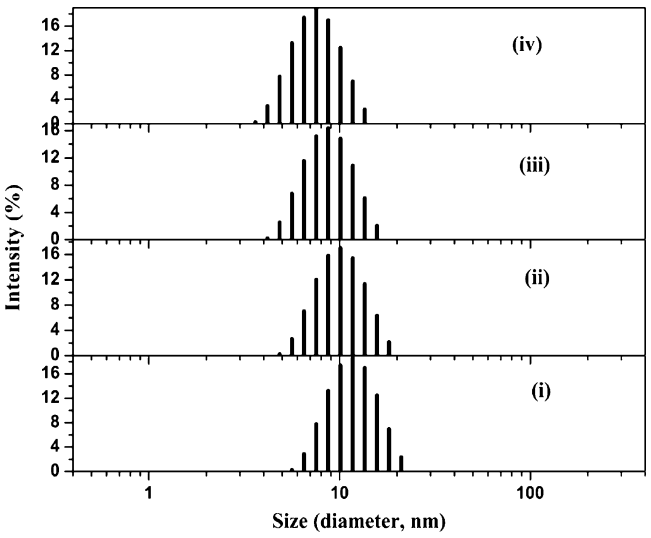

Figure 2. Dynamic light scattering results: variation in size of [Py][TF_2N]/[C_4mim][AOT]/benzene microemulsions (*R* = 0.69) with temperature, (i) 288 K, (ii) 298 K, (iii) 313 K, and (iv) 323 K.

dynamic light scattering measurements (Figure 2) that the microemulsions are monodisperse in nature and the size of the microemulsions decreases with increasing temperature. This decrease in size with increase in temperature is well supported by our earlier observations.[93] There we have shown that the size of the [C_4mim][BF_4]/BHDC/benzene microemulsions decreases with an increase in temperature.[93] The slight decrease in size with temperature clearly indicates the noninteracting hard sphere nature of the [Py][TF_2N]/[C_4mim][AOT]/benzene microemulsions at *R* = 0.69 and absence of any droplet coalescing process.[22,94] In other words the microemulsions retain their structural integrity across the temperature range used in the study.

3.3. Steady State Studies. To determine the location of the probe molecule (C-153) inside the microemulsions, we have recorded absorption and emission spectra of C-153 in neat [Py][TF_2N] and in [Py][TF_2N]/[C_4mim][AOT]/benzene microemulsions at different *R* values. In neat benzene, C-153 shows absorption and emission maximum at 407 and 482 nm, respectively (Table 1). With the addition of [C_4mim][AOT]

Table 1. Steady State Absorption and Emission maxima of C-153 in Benzene, [Py][TF_2N], and [Py][TF_2N]/[C_4mim][AOT]/Benzene Microemulsions at Different *R* Values

system	λ_{max}^{abs} (nm)[a]	λ_{max}^{emi} (nm)[a]
benzene	407	482
[C_4mim][AOT]/benzene	411	508
[Py][TF_2N]/[C_4mim][AOT]/benzene (*R* = 0.14)	413	510
[Py][TF_2N]/[C_4mim][AOT]/benzene (*R* = 0.42)	414	511
[Py][TF_2N]/[C_4mim][AOT]/benzene (*R* = 0.69)	415	512
[Py][TF_2N]/[C_4mim][AOT]/benzene (*R* = 0.95)	417	513
[Py][TF_2N]/[C_4mim][AOT]/benzene (*R* = 1.20)	417	513
[Py][TF_2N]	424	523

[a]Error in experimental data of ±2 nm.

both the absorption and emission maximum get red-shifted to 411 and 508 nm, respectively. This red shift of 26 nm in the emission spectra clearly indicates that the probe molecules are shifted from benzene to the polar interior of the [C_4mim]-[AOT]/benzene reverse micelle. With further addition of [Py][TF_2N] to [C_4mim][AOT]/benzene reverse micelle, we observed a red shift of 6 and 5 nm in the case of absorption and emission spectra of C-153, respectively (Figure 3). This indicates the movement of probe molecules toward the polar IL-pool of the microemulsions. A close inspection of both the absorption and emission spectra (Figure 3) indicates that the absorbance value at the red end of the absorption spectra increases quite rapidly with increasing *R* value (Figure 3a), whereas the emission intensity at the blue end of the emission spectra decreases quite rapidly with increasing *R* value (Figure 3b). These observations give a clear indication that, with the addition of IL ([Py][TF_2N]) to the [C_4mim][AOT]/benzene reverse micelle, the population of the probe molecule (C-153) in benzene decreases and the population of C-153 in IL-pool of the microemulsion increases. We have also monitored the effect of temperature on the emission spectra of C-153 in neat [Py][TF_2N] and in [Py][TF_2N]/[C_4mim][AOT]/benzene microemulsions at *R* = 0.69. We found that the peak maxima and the nature of the emission spectra remain almost same with slight variation in intensity (Figure S1 of Supporting Information). This indicates that the location of the probe molecules is almost unaffected by changes in experimental temperature.

3.4. Time-Resolved Studies. *3.4.1. Time-Resolved Anisotropy Studies.* Absorption and emission spectra provide useful information regarding the location of the probe molecules (C-153) in [Py][TF_2N]/[C_4mim][AOT]/benzene microemulsions and the movement of the probe molecules toward the IL-pool of the microemulsions with increasing *R* value. To support this and to monitor the effect of this movement on the rotational relaxation of C-153, we have recorded its fluorescence anisotropy decay. Being directly related to the reorientation dynamics of excited molecule, the fluorescence anisotropy decay is the best suited technique for investigation of molecular dynamics near the site of dye molecule. Time-

dx.doi.org/10.1021/jp304668f | J. Phys. Chem. B 2012, 116, 8210−8221

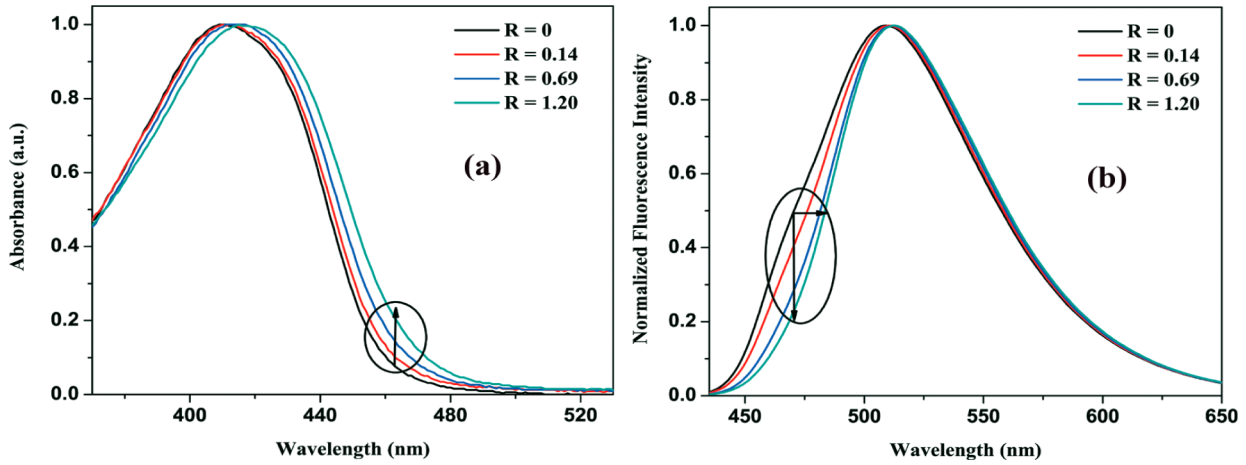

Figure 3. (a) Absorption spectra and (b) emission spectra of C-153 in $[Py][TF_2N]/[C_4mim][AOT]$/benzene microemulsions at different R values.

resolved fluorescence anisotropy $r(t)$ is calculated using the following equation

$$r(t) = \frac{I_{\parallel}(t) - GI_{\perp}(t)}{I_{\parallel}(t) + 2GI_{\perp}(t)} \quad (2)$$

where G is the correction factor for detector sensitivity to the polarization direction of emission and $I_{\parallel}(t)$ and $I_{\perp}(t)$ are fluorescence decays polarized parallel and perpendicular to the polarization of the excitation light, respectively.

The variation of anisotropy decay with increasing R value is shown in Figure 4. The anisotropy decay of C-153 in $[C_4mim][AOT]$/benzene reverse micelle is found to be quite fast and single exponential in nature with a time constant of 0.16 ns. With the addition of ionic liquid, $[Py][TF_2N]$ to the $[C_4mim][AOT]$/benzene reverse micelle the average rotational relaxation time increases, with the emergence of additional slow component (biexponential in nature, Table 2). The average rotational relaxation time of C-153 in $[Py][TF_2N]/[C_4mim][AOT]$/benzene microemulsions at R = 0.14 (at 298 K) is found to be 0.32 ns with components 0.15 ns (95%) and 3.56 ns (5%). This biexponential nature clearly indicates that the probe molecule senses two quite different regions inside the microemulsions: a fast region near the headgroup of $[C_4mim][AOT]$ surfactant and a slow region in the IL pool inside the microemulsion. This observation also supports the movement of probe molecule to IL-pool of the microemulsions. The slow component of rotational decay of C-153 in $[Py][TF_2N]/[C_4mim][AOT]$/benzene microemulsions at R = 0.14 (3.56 ns) is higher compared to that in neat IL, $[Py][TF_2N]$ (2.86 ns). This higher value arises due to the presence of additional confinement in the microemulsion. With further addition of IL, i.e., with increasing R value from 0.14 to 1.20 the average rotational relaxation time of C-153 in $[Py][TF_2N]/[C_4mim][AOT]$/benzene microemulsions increases from 0.32 to 0.39 ns (Table 2). This increase in average rotational relaxation time with increase in R value can be accounted for by the movement of probe molecule toward IL-pool of the microemulsions. So, we can say that the probe molecule senses high microviscosity with the movement toward the IL-pool of the microemulsions. We have also monitored the effect of temperature on the fluorescence anisotropy decay of C-153 in neat $[Py][TF_2N]$ and in $[Py][TF_2N]/[C_4mim][AOT]$/benzene microemulsions at R = 0.69. The representative anisotropy decays are shown in Figure 5. The anisotropy decays of C-153 in $[Py][TF_2N]/[C_4mim][AOT]$/benzene microemulsions are found to be biexponential in nature at all the experimental temperatures and are less sensitive to the temperature compared to that in neat $[Py][TF_2N]$ (Table 3). With the increase of temperature from 288 to 323 K the average rotational relaxation time of C-153 in $[Py][TF_2N]/[C_4mim][AOT]$/benzene microemulsions gradu-

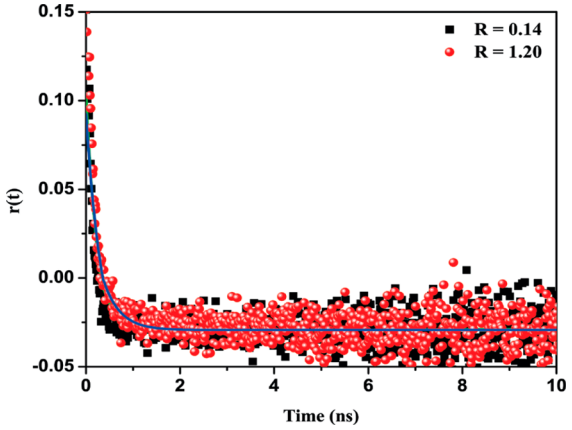

Figure 4. Anisotropy decays of C-153 in $[Py][TF_2N]/[C_4mim][AOT]$/benzene microemulsions at different R values at 298 K.

Table 2. Anisotropy Decay Parameters of C-153 in $[Py][TF_2N]/[C_4mim][AOT]$/Benzene Microemulsions at Different R Values

system	a_{fast}	τ_1 (ns)	a_{slow}	τ_2 (ns)	$\langle\tau_{rot}\rangle^a$ (ns)
$[Py][TF_2N]/[C_4mim][AOT]$/benzene ($R$ = 0.14)	0.95	0.15	0.05	3.56	0.32
$[Py][TF_2N]/[C_4mim][AOT]$/benzene ($R$ = 0.69)	0.94	0.15	0.06	3.62	0.36
$[Py][TF_2N]/[C_4mim][AOT]$/benzene ($R$ = 1.20)	0.94	0.17	0.06	3.83	0.39

[a]Experimental error of ±5%.

dx.doi.org/10.1021/jp304668f | J. Phys. Chem. B 2012, 116, 8210−8221

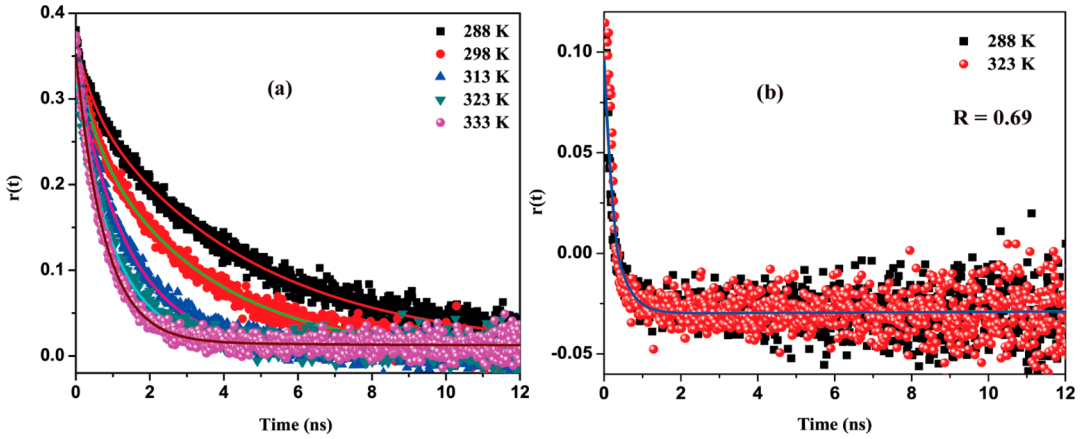

Figure 5. (a) Anisotropy decays of C-153 in neat [Py][TF_2N] at different temperatures and (b) anisotropy decays of C-153 in [Py][TF_2N]/[C_4mim][AOT]/benzene microemulsions (R = 0.69) at different temperatures.

Table 3. Anisotropy Decay Parameters of C-153 in Neat [Py][TF_2N] and [Py][TF_2N]/[C_4mim][AOT]/Benzene (R = 0.69) Microemulsions at Different Temperatures

system	temp (K)	a_{fast}	τ_1 (ns)	a_{slow}	τ_2 (ns)	$\langle\tau_{rot}\rangle^a$ (ns)	viscosity (cP)
[Py][TF_2N]/[C_4mim][AOT]/benzene (R = 0.69)	288	0.93	0.17	0.07	3.75	0.42	1.44 ± 0.04
	298	0.94	0.15	0.06	3.62	0.36	1.12 ± 0.03
	313	0.94	0.11	0.06	3.18	0.29	0.78 ± 0.03
	323	0.95	0.11	0.05	2.80	0.24	0.56 ± 0.02
[Py][TF_2N]	288	0.18	0.32	0.82	4.05	3.38	83.48 ± 2.89
	298	0.19	0.27	0.81	2.86	2.37	52.54 ± 2.53
	313	0.15	0.23	0.85	1.60	1.39	29.36 ± 1.82
	323	0.15	0.14	0.85	1.11	0.96	21.06 ± 1.24
	333	0.16	0.12	0.84	0.83	0.72	17.47 ± 1.20

[a]Experimental error of ±5%.

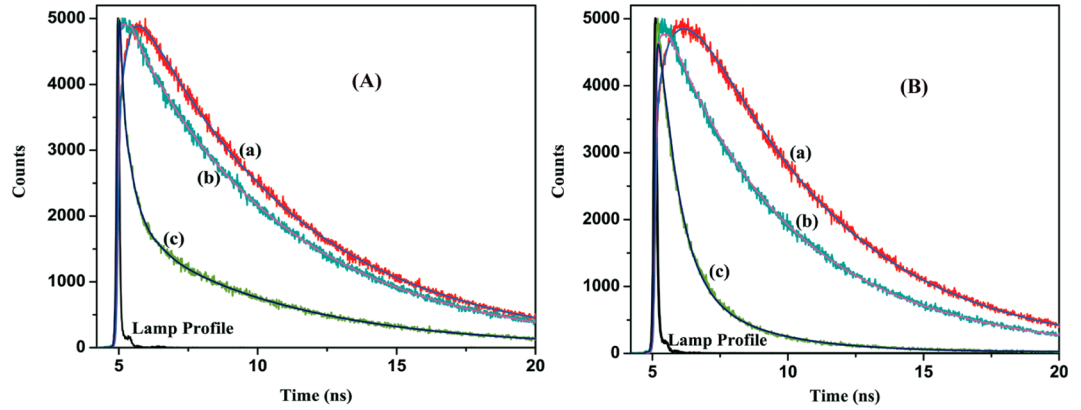

Figure 6. Fluorescence decays of C-153 at 298 K in (A) neat [Py][TF_2N] at (a) 610 nm, (b) 523 nm, and (c) 485 nm. (B) [Py][TF_2N]/[C_4mim][AOT]/benzene microemulsions (R = 0.69) at (a) 580 nm, (b) 512 nm, and (c) 460 nm.

ally changes from 0.42 to 0.24 ns, respectively (1.75 times decrease), whereas in the case of neat [Py][TF_2N] it changes from 3.38 to 0.96 ns, respectively (3.52 times decrease). The decrease in average rotational relaxation time clearly indicates that the probe molecule becomes free to rotate at elevated temperatures. The difference in the extent of change in average rotational relaxation time of the probe molecule arises due to the difference in behavior of neat IL and IL in microemulsions.[92,93,95,96] Interestingly, the effect of both increasing R value and increasing temperature on average rotational relaxation time of C-153 in [Py][TF_2N]/[C_4mim][AOT]/benzene microemulsions shows a similar trend with our earlier characterized systems namely C-153/C-480 in [Py][TF_2N]/TX-100/benzene[92] and C-480 in [C_4mim][BF_4]/BHDC/benzene microemulsions.[93]

3.4.2. Solvation Dynamics. We have gathered information regarding location of the probe molecule (C-153) inside the [Py][TF_2N]/[C_4mim][AOT]/benzene microemulsions by absorption and emission spectroscopy. The fluorescence anisotropy decay measurements reveal information about the reorientational dynamics of excited probe molecule. To study the solvent relaxation dynamics (solvation dynamics), we have used C-153 as the probe molecule. We collected the time-resolved fluorescence decays of C-153 monitored at different

dx.doi.org/10.1021/jp304668f | J. Phys. Chem. B 2012, 116, 8210−8221

wavelengths for all the systems. The fluorescence decays of C-153 showed huge dependence on the emission wavelength in every system studied. At the red edge of emission spectra, the observed decay consists of a clear rise (growth) followed by usual decay, and at the blue end of emission spectra, a faster decay is observed which is a clear signature of the solvation dynamics. The representative decays of C-153 in neat [Py][TF_2N] and in [Py][TF_2N]/[C_4mim][AOT]/benzene microemulsion (R = 0.69) monitoring at three different wavelengths at 298 K are shown in Figure 6. The red edge and extreme blue edge decay profiles were best fitted by biexponential and triexponential functions, respectively. The time-resolved emission spectra (TRES) were constructed by the following procedure of Fleming and Maroncelli.[97,98] The TRES at a given time t, $S(\lambda;t)$, is obtained by the fitted decays, $D(t;\lambda)$, by relative normalization to the steady state spectrum $S_0(\lambda)$, as follows

$$S(\lambda;t) = D(t;\lambda)\frac{S_0(\lambda)}{\int_0^\infty D(t;\lambda)\,dt} \tag{3}$$

Each time-resolved emission spectrum (TRES) was fitted by "log-normal line shape function", which is defined as

$$g(\nu) = g_0 \exp\left[-\ln 2\left(\frac{\ln[1 + 2b(\nu - \nu_p)/\Delta]}{b}\right)^2\right] \tag{4}$$

where g_0, b, ν_p, and Δ are the peak height, asymmetric parameter, peak frequency, and width parameter, respectively. The representative TRES plot of C-153 in neat [Py][TF_2N] and in [Py][TF_2N]/[C_4mim][AOT]/benzene microemulsion (R = 0.69) at 298 K are shown in Figure S2 of the Supporting Information. The peak frequency evaluated from this log-normal fitting of TRES was then used to construct the decay of the solvent correlation function $C(t)$, which is defined as

$$C(t) = \frac{\nu(t) - \nu(\infty)}{\nu(0) - \nu(\infty)} \tag{5}$$

$\nu(0)$ is the frequency at "zero-time", as calculated by the full method of Fleming and Maroncelli.[97] $\nu(\infty)$ is the frequency at "infinite time", which may be taken as the maximum of the steady state fluorescence spectrum if solvation is more rapid than the population decay of the probe. $\nu(t)$ is determined by taking the maxima from the log-normal fits as the emission maximum. In most of the cases, however, the spectra are broad, so there is some uncertainty in the exact position of the emission maxima. Therefore, we have considered the range of the raw data points in the neighborhood of the maximum to estimate an error for the maximum obtained from the log-normal fit as suggested by Petrich et al.[99−101] Depending on the width of the spectrum (i.e., zero-time, steady state, or TRES), we have determined the typical uncertainties as follows: zero time ≈ steady state (100 cm^{-1}) < timeresolved (190 cm^{-1}) emission. We use these uncertainties to compute error bars for $C(t)$. Finally, in generating $C(t)$, the first point was obtained from the zero time spectrum. The second point was taken at the maximum of the instrument response function, which, having a full width at half-maximum of ≤100 ps, was taken to be 100 ps. Finally, the time dependence of the calculated $C(t)$ values were fitted by a biexponential function because χ^2 lies close to 1, which indicates the goodness of the fit. The biexponential function is as follows

$$C(t) = a_1 e^{-t/\tau_1} + a_2 e^{-t/\tau_2} \tag{6}$$

where τ_1 and τ_2 are the two solvation times (≥100 ps, below this we are missing owing to our instrumental resolution) with amplitudes of a_1 and a_2, respectively. The missing component can be defined as $(1 - (a_1 + a_2)) \times 100\%$. The $C(t)$ versus time plots for [Py][TF_2N]/[C_4mim][AOT]/benzene microemulsions at different R values are shown in Figure 7. The decay

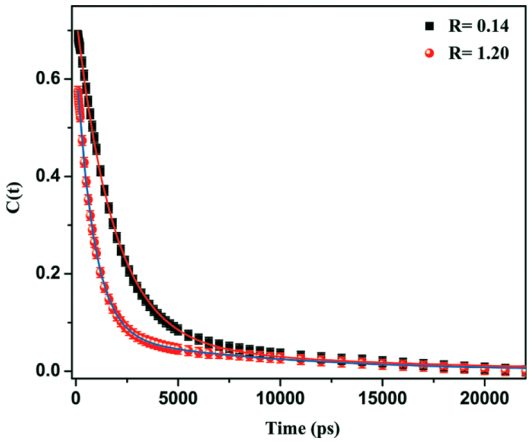

Figure 7. Decays of solvent correlation functions $C(t)$ of C-153 in [Py][TF_2N]/[C_4mim][AOT]/benzene microemulsions at different R values at 298 K.

parameters of $C(t)$ of C-153 in [Py][TF_2N]/[C_4mim][AOT]/benzene microemulsions at different R values are summarized in Table 4. The observed average solvation time is calculated as

$$\tau_{av} = a_1\tau_1 + a_2\tau_2 \tag{7}$$

The average solvation time of C-153 at 298 K in neat [Py][TF_2N] was found to be 0.19 ns (Table 4) with components 0.31 ns (28.0%) and 0.66 ns (16.0%). The average solvation time in neat [Py][TF_2N] differs from the average solvation time reported in our earlier manuscript.[92] This difference arises due to the difference in the construction of C(t) (in our earlier manuscript we have not excluded the missing component). The observed time constants change drastically when [Py][TF_2N] is incorporated inside the [C_4mim][AOT]/benzene reverse micelle. The average solvation time of C-153 at 298 K in [Py][TF_2N]/[C_4mim][AOT]/benzene microemulsion at R = 0.14 was found to be 1.97 ns (Table 4) with components 1.83 ns (67.1%) and 11.81 ns (6.3%). So the average solvation time increases by a factor of ∼10 with incorporation of IL in reverse micelle. Similar behavior has been observed when [Py][TF_2N] is incorporated inside the TX-100/benzene reverse micelle.[92] This increase in average solvation time can be explained by considering the effect of nano confinement and different interactions with the surfactant headgroup. The biexponential nature of solvation dynamics in [Py][TF_2N]/[C_4mim][AOT]/benzene microemulsions with increased time constants compared to that of neat [Py][TF_2N] originates from the presence of two different types of IL molecules inside the microemulsions. The first type are the IL molecules present around the probe molecule and are located near the headgroup of [C_4mim][AOT] surfactant whereas the other types are those IL molecules present slightly

dx.doi.org/10.1021/jp304668f | J. Phys. Chem. B 2012, 116, 8210−8221

Table 4. Decay Parameters of $C(t)$ of C-153 in Neat [Py][TF_2N] and [Py][TF_2N]/[C_4mim][AOT]/Benzene Microemulsions at Different R Values (Excluding Missing Component)

system	τ_i (a_i) (ns)	$\langle\tau_s\rangle^a$ (ns)	viscosity (cP)	diameter (nm)	missing component (%)
[Py][TF_2N]/[C_4mim][AOT]/benzene (R = 0.14)	1.83 (0.671), 11.81 (0.063)	1.97	0.87 ± 0.02	4.2 ± 0.2	26.6
[Py][TF_2N]/[C_4mim][AOT]/benzene (R = 0.42)	1.26 (0.629), 10.29 (0.074)	1.55	0.98 ± 0.02	6.5 ± 0.3	29.7
[Py][TF_2N]/[C_4mim][AOT]/benzene (R = 0.69)	0.94 (0.612), 9.45 (0.075)	1.28	1.12 ± 0.03	10.2 ± 0.5	31.3
[Py][TF_2N]/[C_4mim][AOT]/benzene (R = 0.95)	0.85 (0.591), 9.07 (0.078)	1.21	1.38 ± 0.03	15.9 ± 0.8	33.1
[Py][TF_2N]/[C_4mim][AOT]/benzene (R = 1.20)	0.85 (0.564), 8.79 (0.078)	1.17	1.97 ± 0.04	41.2 ± 2.1	35.8
[Py][TF_2N]	0.31 (0.280), 0.66 (0.160)	0.19	52.54 ± 2.53		56.0

[a]Experimental error of ±0.09 ns. $\langle\tau_s\rangle = a_1\tau_1 + a_2\tau_2$, τ_i < 100 ps is missing owing to our instrumental resolution.

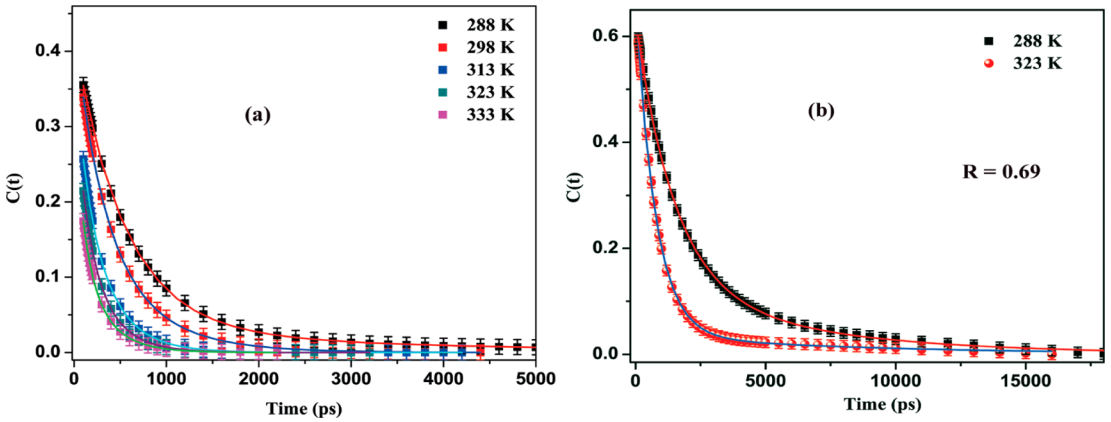

Figure 8. Decays of solvent correlation functions $C(t)$ of C-153 in (a) neat [Py][TF_2N] at different temperatures and (b) [Py][TF_2N]/[C_4mim][AOT]/benzene microemulsions (R = 0.69) at different temperatures.

away from the probe molecule and are located in the core of the IL pool inside the microemulsion. The RTIL molecules present near the surfactant headgroup, i.e., at the interfacial regions, feel much more restricted environment compared to those present in the IL pool of the microemulsions. So the RTIL molecules present at the interfacial regions contribute to the slow component and the RTIL molecules present away from surfactants molecules contribute to the fast component of solvation dynamics. Interestingly, the increase in average solvation time on going from neat water to water-containing microemulsions (which is of the order of 100−1000 times[15,46,51,52,54,58]) is quite high compared to the increase in average solvation time on going from neat IL to IL-containing microemulsions (which is of the order of ∼10 times). The huge retardation of solvation dynamics in case of the former arises due to extended hydrogen bonding between water and surfactant molecules, counterions, and the micellar head groups. Recent computer simulation[102] studies have shown that the hydrogen bonding between water molecules and surfactant is much stronger than the hydrogen bond between the two water molecules. On the other hand, the small retardation of solvation dynamics on going from neat IL to IL-containing microemulsions suggests that the movement of cation and anion of RTIL is only slightly affected by the confinement. In other words we can say that (1) the microemulsions formation has little effect on the interaction between the ions of RTILs and (2) the interaction between the surfactant and the RTIL is almost same as the interaction between the ions of RTILs (both electrostatic in nature).

With gradual increase in R value (i.e., with gradual loading of IL) from 0.14 to 1.20 the average solvation time decreases from 1.97 to 1.17 ns (1.68 times). A gradual decrease in both slow and fast components is observed with increasing R value. The slow component decreases from 11.81 to 8.79 ns, whereas the fast component decreases from 1.83 to 0.85 ns with an increase in R value from 0.14 to 1.20. This regular decrease of both slow and fast components of solvation dynamics is a manifestation of the regular increase in the size of the microemulsions (Table 4). With the increase in the size of the microemulsions, the RTIL becomes less confined and can move freely. A close inspection of the observed size increase with increase in R value of the microemulsions and corresponding decrease in average solvation time indicates that the solvation dynamics of C-153 in [Py][TF_2N]/[C_4mim][AOT]/benzene microemulsions exhibits small R dependence. This small R dependence is further supported by our earlier observations. We have shown that with gradual increase of R value from 0.23 to 0.69 in case of [Py][TF_2N]/TX-100/benzene microemulsions the average solvation times of C-153 and C-480 decreases by factors of 1.34 and 1.62, respectively.[92] This behavior is entirely different from that observed in case of reverse micelles containing hydrogen bond-forming solvents, e.g., water,[53] methanol,[24] glycerol,[103] and dimethylformamide (DMF).[104] In fact, it is similar to the results obtained from reverse micelles containing solvents incapable of hydrogen bonding, e.g., acetonitrile[24] and DMF.[104] Shirota et al.[104] have also observed that the aprotic dimethylformamide (DMF)-containing reverse micelles showed a small R dependence in contrast to protic formamide (FA)-containing reverse micelles, which show strong R dependence of the solvation dynamics. So, the absence of hydrogen bonding within the IL is the origin of this small R dependence.

We have also monitored the effect of temperature on the solvation dynamics of C-153 in neat [Py][TF_2N] and [Py][TF_2N]/[C_4mim][AOT]/benzene microemulsions. The $C(t)$ versus time plots for neat [Py][TF_2N] and in [Py]-

dx.doi.org/10.1021/jp304668f | J. Phys. Chem. B 2012, 116, 8210−8221

Table 5. Decay Parameters of $C(t)$ of C-153 in Neat [Py][TF_2N] and [Py][TF_2N]/[C_4mim][AOT]/Benzene (R = 0.69) Microemulsions at Different Temperatures (Excluding Missing Component)

system	temp (K)	τ_i (a_i) (ns)	$\langle\tau_s\rangle^a$ (ns)	missing component (%)
[Py][TF_2N]/[C_4mim][AOT]/benzene (R = 0.69)	288	1.49 (0.503), 9.84 (0.093)	1.66	40.4
	298	0.94 (0.612), 9.45 (0.075)	1.28	31.3
	313	0.82 (0.623), 9.00 (0.062)	1.07	31.5
	323	0.75 (0.640), 8.40 (0.037)	0.79	32.3
[Py][TF_2N]	288	0.53 (0.388), 3.13 (0.030)	0.30	58.2
	298	0.31 (0.280), 0.66 (0.160)	0.19	56.0
	313	0.16 (0.153), 0.34 (0.233)	0.10	61.4
	323	0.14 (0.188), 0.32 (0.165)	0.08	64.7
	333	0.11 (0.183), 0.30 (0.140)	0.06	67.7

[a]Experimental error of ±0.09 ns. $\langle\tau_s\rangle = a_1\tau_1 + a_2\tau_2$, τ_i < 100 ps is missing owing to our instrumental resolution.

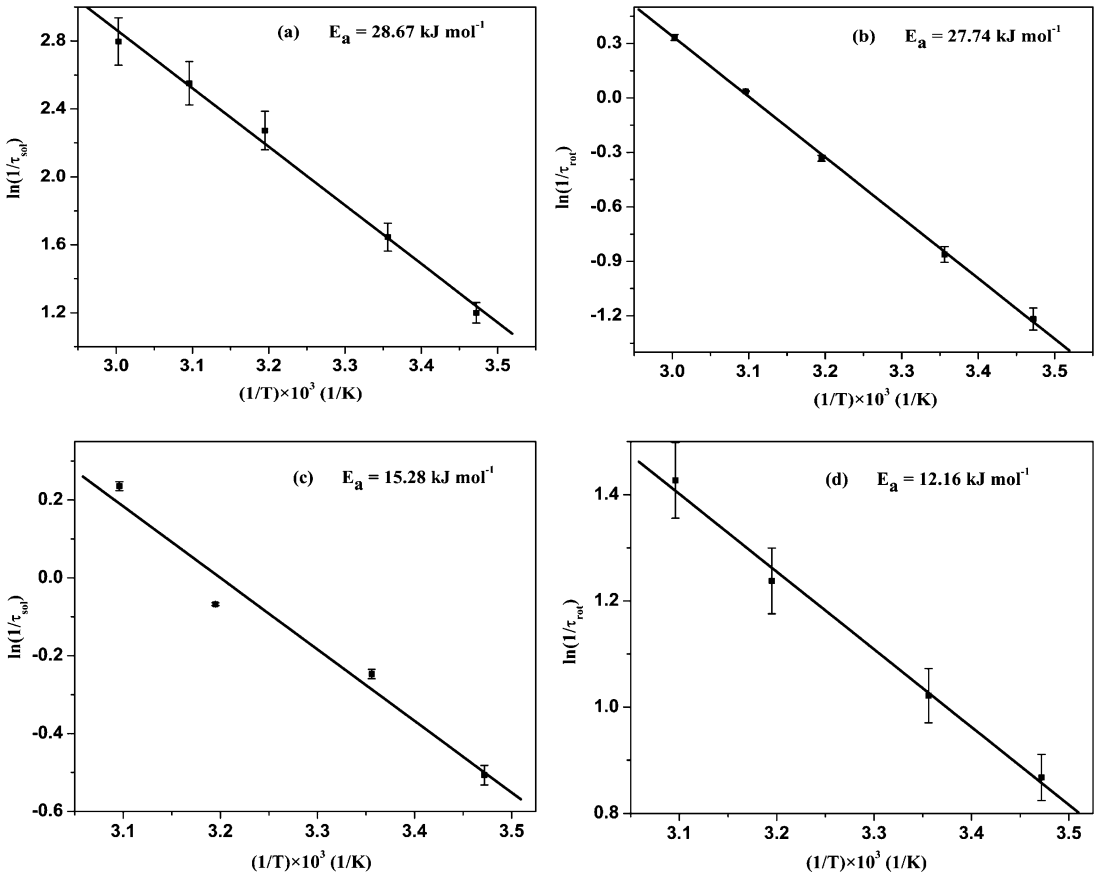

Figure 9. Plots of $\ln(1/\tau_{sol})$ and $\ln(1/\tau_{rot})$ against $1/T$ in (a, b) neat [Py][TF_2N] and (c, d) [Py][TF_2N]/[C_4mim][AOT]/benzene microemulsions at R = 0.69.

[TF_2N]/[C_4mim][AOT]/benzene microemulsion (R = 0.69) at different temperatures are shown in Figure 8. The decay parameters of $C(t)$ of C-153 in neat [Py][TF_2N] and in [Py][TF_2N]/[C_4mim][AOT]/benzene microemulsion (R = 0.69) at different temperatures are summarized in Table 5. With the gradual increase in temperature from 288 to 323 K the average solvation time of C-153 in [Py][TF_2N]/[C_4mim]-[AOT]/benzene microemulsions decreases from 1.66 to 0.79 ns (Table 5). A gradual decrease in both slow and fast components is observed with increasing temperature. The slow component decreases from 9.84 to 8.40 ns, whereas the fast component decreases from 1.49 to 0.75 ns with an increase in temperature from 288 to 323 K. This regular decrease in both the components of average solvation time indicates that an increase in temperature accelerates the solvation process at the interface and IL-pool irrespective of the microemulsion size. We also found that the solvation dynamics in neat [Py][TF_2N] is affected substantially by the temperature; however, for the [Py][TF_2N]/[C_4mim][AOT]/benzene microemulsions the temperature effect on the solvation dynamics is not that significant. In other words, the diffusional motion of the constituents of the IL in microemulsion is less susceptible to temperature changes compared to that in neat IL. This is once again due to the difference in behavior of neat IL and IL in microemulsions.[92,93,95,96]

3.5. Activation Energy. A careful analysis of the temperature dependence of average solvation time and rotational relaxation time can be used to calculate the activation energies (E_a) associated with these processes in neat [Py]-[TF_2N] and in [Py][TF_2N]/[C_4mim][AOT]/benzene micro-

dx.doi.org/10.1021/jp304668f | J. Phys. Chem. B 2012, 116, 8210−8221

emulsions. Assuming traditional Arrhenius dependence of the rate constants ($1/\tau$), the activation energies (E_a) have been evaluated from the logarithmic plot of $1/\tau$ against $1/T$ (Figure 9).[105] The activation energy (E_a) obtained from the average solvation and rotational relaxation time for neat [Py][TF_2N] are 28.67 and 27.74 kJ/mol, respectively. On the other hand, the activation energy (E_a) obtained from the average solvation and rotational relaxation time for [Py][TF_2N]/[C_4mim][AOT]/benzene microemulsions (R = 0.69) are 15.28 and 12.16 kJ/mol, respectively. Similar behavior was observed in case of [C_4mim][BF_4]/BHDC/benzene microemulsions.[93] The E_a obtained from the average solvation times for neat [C_4mim][BF_4] and [C_4mim][BF_4] in [C_4mim][BF_4]/BHDC/benzene microemulsions are 33.65 and 18.28 kJ/mol, respectively.[93] The larger value of activation energy in the case of neat IL compared to that of IL-containing microemulsions clearly indicates the stronger temperature dependence of solvation and rotational relaxation dynamics in case of the former system compared to the latter. In other words we can say that the diffusional motion of the constituents of the RTIL (which is responsible for the solvation dynamics) show more temperature dependence in the case of neat IL, [Py][TF_2N] compared to that in [Py][TF_2N]-containing microemulsions.

4. CONCLUSION

For the first time we have explored the solvent and rotational relaxation dynamics of C-153 in ionic liquid-in-oil microemulsions composed of double chain surface active ionic liquid ([C_4mim][AOT]) as a surfactant and RTIL ([Py][TF_2N]) as the polar core. We can conclusively state that the electrostatic interaction between the constituents of the IL remains almost same on incorporation in microemulsions. This leads to a small increase in average solvation time (~10 times) compared to the increase observed on going from pure water to water-containing microemulsions (100−1000 times). The average solvation and rotational relaxation time shows small R dependence. The average solvation time decreases with increasing R values, which can be ascribed to the movement of C-153 molecule from the interfacial region of [C_4mim][AOT]/benzene to the polar core of microemulsions. This movement of C-153 is well supported by a red shift in absorption and emission spectra. In contrast to aqueous microemulsions these systems exhibited low temperature dependence. The observed stronger temperature dependence of the solvation dynamics in the case of neat [Py][TF_2N] compared to that of [Py][TF_2N]-containing microemulsions can be explained by the fact that electrostatic interaction (between the negatively charged AOT^- group of the surfactant and the RTIL which acts as the polar core) is the chief stabilizing interaction within the microemulsions. Interestingly, the small increase in average solvation time (~10 times), small R dependence, and low temperature dependence of the average solvation and rotational relaxation time, was also shown by our earlier characterized systems, e.g., C-153/C-480 in [Py][TF_2N]/TX-100/benzene[92] and C-480 in [C_4mim][BF_4]/BHDC/benzene microemulsions.[93] So we can conclude that the nature and strength of interactions within the polar solvents (molecular solvents or ionic liquids) and the interactions within polar solvents and surfactants molecule is the main determining factor for the determination of change in solvation and rotational dynamics. Characterization of this type of microemulsion can be advantageous in many ways. Zech et al.[42] have shown that microemulsions consisting of cationic surface active ionic liquid as a surfactant and IL, as a polar phase were stable within a temperature range between 30 and 150 °C. In our case also the microemulsion consists of anionic double chain surface active ionic liquid ([C_4mim][AOT]) as a surfactant and IL ([Py][TF_2N]) as a polar phase, so it can find various applications at high temperature if we choose a nonpolar solvent of high boiling point. Also, in our earlier manuscript we have shown how a huge number of reverse IL-in-oil microemulsions can be formulated. So if we can replace benzene by a nonpolar solvent of high boiling point, then we can have a large number of microemulsions that will exhibit stability over a wide range of temperature.

■ ASSOCIATED CONTENT

Ⓢ Supporting Information

Effect of temperature on emission spectra and TRES plots. This material is available free of charge via the Internet at http://pubs.acs.org.

■ AUTHOR INFORMATION

Corresponding Author

*E-mail: nilmoni@chem.iitkgp.ernet.in. Fax: 91-3222-255303.

Notes

The authors declare no competing financial interest.

■ ACKNOWLEDGMENTS

N.S. thanks the Council of Scientific and Industrial Research (CSIR), and Board of Research in Nuclear Sciences (BRNS), Government of India, for generous research grants. V.G.R., S.M., and S.G. are thankful to CSIR, and C.B. is thankful to UGC for a research fellowship. We are thankful to Ms. Udita Brahmachari for English correction of this manuscript.

■ REFERENCES

(1) Johnston, K. P.; Harrison, K. L.; Clarke, M. J.; Howdle, S. M.; Heitz, M. P.; Bright, F. V.; Carlier, C.; Randolph, T. W. *Science* **1996**, *271*, 624−626.
(2) Eastoe, J.; Gold, S.; Rogers, S.; Wyatt, P.; Steytler, D. C.; Gurgel, A.; Heenan, R. K.; Fan, X.; Beckman, E. J.; Enick, R. M. *Angew. Chem., Int. Ed.* **2006**, *45*, 3675−3677.
(3) Liu, Y.; Jessop, P. G.; Cunningham, M.; Eckert, C. A.; Liotta, C. L. *Science* **2006**, *313*, 958−960.
(4) Oh, S.; Kizling, J.; Holmberg, K. *Colloid Surf. A* **1995**, *97*, 169−179.
(5) Wagner, G. W.; Procell, L. R.; Yang, Y.-Chu; Bunton, C. A. *Langmuir* **2001**, *17*, 4809−4811.
(6) Bonini, M.; Bardi, U.; Berti, D.; Neto, C.; Baglioni, P. *J. Phys. Chem. B* **2002**, *106*, 6178−6183.
(7) Lv, F. F.; Zheng, L. Q.; Tung, C. *Int. J. Pharm.* **2005**, *301*, 237−246.
(8) Mandal, D.; Datta, A.; Pal, S. K.; Bhattacharyya, K. *J. Phys. Chem. B* **1998**, *102*, 9070−9073.
(9) Dutta, P.; Sen, P.; Mukherjee, S.; Halder, A.; Bhattacharyya, K. *J. Phys. Chem. B* **2003**, *107*, 10815−10822.
(10) Novaira, M.; Biasutti, M. A.; Silber, J. J.; Correa, N. M. *J. Phys. Chem. B* **2007**, *111*, 748−759.
(11) Agazzi, F. M.; Falcone, R. D.; Silber, J. J.; Correa, N. M. *J. Phys. Chem. B* **2011**, *115*, 12076−12084.
(12) Nave, S.; Eastoe, J.; Heenan, R. K.; Steytler, D.; Grillo, I. *Langmuir* **2000**, *16*, 8741−8748.
(13) Angelico, R.; Ceglie, A.; Colafemmina, G.; Delfine, F.; Olsson, U.; Palazzo, G. *Langmuir* **2004**, *20*, 619−631.
(14) Piletic, I. R.; Moilanen, D. E.; Levinger, N. E.; Fayer, M. D. *J. Am. Chem. Soc.* **2006**, *128*, 10366−10367.

(15) Baruah, B.; Roden, J. M.; Sedgwick, M.; Correa, N. M.; Crans, D. C.; Levinger, N. E. *J. Am. Chem. Soc.* **2006**, *128*, 12758−12765.
(16) Gao, H. X.; Li, J. C.; Han, B. X.; Chen, W. N.; Zhang, J. L.; Zhang, R.; Yan, D. D. *Phys. Chem. Chem. Phys.* **2004**, *6*, 2914−2916.
(17) Eastoe, S.; Gold, S. E.; Rogers, A.; Paul, T.; Welton, R. K.; Heenan, I. G. *J. Am. Chem. Soc.* **2005**, *127*, 7302−7303.
(18) Chakrabarty, D.; Seth, D.; Chakraborty, A.; Sarkar, N. *J. Phys. Chem. B* **2005**, *109*, 5753−5758.
(19) Gao, Y. A.; Zhang, J.; Xu, H. Y.; Zhao, X. Y.; Zheng, L. Q.; Li, X. W.; Yu, L. *ChemPhysChem* **2006**, *7*, 1554−1561.
(20) Li, N.; Gao, Y. A.; Zheng, L. Q.; Zhang, J.; Yu, L.; Li, X. W. *Langmuir* **2007**, *23*, 1091−1097.
(21) Gao, Y. A.; Li, N.; Zheng, L. Q.; Bai, X. T.; Yu, L.; Zhao, X. Y.; Zhang, J.; Zhao, M. W.; Li, Z. *J. Phys. Chem. B.* **2007**, *111*, 2506−2513.
(22) Falcone, R. D.; Correa, N. M.; Silber, J. J. *Langmuir* **2009**, *25*, 10426−10429.
(23) Correa, N. M.; Pires, P. A. R.; Silber, J. J. A.; El Seoud, O. *J. Phys. Chem. B* **2005**, *109*, 21209−21219.
(24) Shirota, H.; Horie, K. *J. Phys. Chem. B* **1999**, *103*, 1437−1443.
(25) Das, K. P.; Ceglie, A.; Lindman, B. *J. Phys. Chem.* **1987**, *91*, 2938−2946.
(26) Schubert, K. V.; Lusvardi, K. M.; Kaler, E. W. *Colloid Interface Sci.* **1996**, *274*, 875−883.
(27) Ray, S.; Moulik, S. P. *Langmuir* **1994**, *10*, 2511−2515.
(28) Ranke, J.; Stolte, S.; Stormann, R.; Arning, J.; Jastorff, B. *Chem. Rev.* **2007**, *107*, 2183−2206.
(29) Fletcher, K. A.; Pandey, S. *Langmuir* **2004**, *20*, 33−36.
(30) Rai, R.; Baker, G. A.; Behera, K.; Mohanty, P.; Kurur, N. D.; Pandey, S. *Langmuir* **2010**, *26*, 17821−17826.
(31) Behera, K.; Om, H.; Pandey, S. *J. Phys. Chem. B* **2009**, *113*, 786−793.
(32) Behera, K.; Pandey, S. *Langmuir* **2008**, *24*, 6462−6469.
(33) Rao, V. G.; Ghatak, C.; Ghosh, S.; Pramanik, R.; Sarkar, S.; Mandal, S.; Sarkar, N. *J. Phys. Chem. B* **2011**, *115*, 3828−3837.
(34) Qiu, Z.; Texter, J. *Curr. Opin. Colloid Interface Sci.* **2008**, *13*, 252−262.
(35) Gao, Y.; Wang, S.; Zheng, L.; Han, S.; Zhang, X.; Lu, D.; Yu, L.; Ji, Y.; Zhang, G. *J. Colloid Interface Sci.* **2006**, *301*, 612−616.
(36) Spiro, M.; de Jesus, D. M. *Langmuir* **2000**, *16*, 2464−2468.
(37) Gayet, F.; El Kalamouni, C.; Lavedan, P.; Marty, J. D.; Brûlet, A.; Lauth-de Viguerie, N. *Langmuir* **2009**, *25*, 9741−9750.
(38) Zhou, Y; Qiu, L.; Deng, Z.; Texter, J.; Yan, F. *Macromolecules* **2011**, *44*, 7948−7955.
(39) Chen, Z.; Yan, F.; Qiu, L.; Lu, J.; Zhou, Y.; Chen, J.; Tang, Y.; Texter, J. *Langmuir* **2010**, *26*, 3803−3806.
(40) Moniruzzaman, M; Tahara, Y.; Tamura, M.; Kamiyaab, N.; Goto, M. *Chem. Commun.* **2010**, *46*, 1452−1454.
(41) Gao, Y.; Li, N.; Hilfert, L.; Zhang, S.; Zheng, L.; Yu, L. *Langmuir* **2009**, *25*, 1360−1365.
(42) Zech, O.; Thomaier, S.; Kolodziejski, A.; Touraud, D.; Grillo, I.; Kunz, W. *Chem.—Eur. J.* **2010**, *16*, 783−786.
(43) Zech, O.; Thomaier, S.; Bauduin, P.; Rück, T.; Touraud, D.; Kunz, W. *J. Phys. Chem. B* **2009**, *113*, 465−473.
(44) A. El Seoud, O.; Pires, P. A. R.; Abdel-Moghny, T.; Bastos, E. L. *J. Colloid Interface Sci.* **2007**, *313*, 296−304.
(45) Inoue, T.; Dong, B.; Zheng, L. Q. *J. Colloid Interface Sci.* **2007**, *307*, 578−581.
(46) Nandi, N.; Bhattacharyya, K.; Bagchi, B. *Chem. Rev.* **2000**, *100*, 2013−2046.
(47) Bagchi, B. *Chem. Rev.* **2005**, *105*, 3197−3219.
(48) Bagchi, B.; Jana, B. *Chem. Soc. Rev.* **2010**, *39*, 1936−1954.
(49) Kumbhakar, M.; Nath, S.; Mukherjee, T.; Pal, H. *J. Chem. Phys.* **2004**, *121*, 6026−6033.
(50) Sen, P.; Mukherjee, S.; Halder, A.; Bhattacharyya, K. *Chem. Phys. Lett.* **2004**, *385*, 357−361.
(51) Willard, D. M.; Riter, R. E.; Levinger, N. E. *J. Am. Chem. Soc.* **1998**, *120*, 4151−4160.
(52) Riter, R. E.; Undiks, E. P.; Levinger, N. E. *J. Am. Chem. Soc.* **1998**, *120*, 6062−6067.
(53) Sarkar, N.; Dutta, A.; Das, S.; Bhattacharyya, K. *J. Phys. Chem.* **1996**, *100*, 10523−10527.
(54) Bhattacharyya, K.; Bagchi, B. *J. Phys. Chem. A* **2000**, *104*, 10603−10613.
(55) Pal, S. K.; Zewail, A. H. *Chem. Rev.* **2004**, *104*, 2099−2124.
(56) Pal, S. K.; Zhao, L.; Zewail, A. H. *Proc. Natl Acad. Sci. USA* **2003**, *100*, 8113−8118.
(57) Nandi, N.; Bagchi, B. *J. Phys. Chem. B* **1997**, *101*, 10954−10961.
(58) Bhattacharyya, K. *Acc. Chem. Res.* **2003**, *36*, 95−101.
(59) Pal, S. K.; Peon, J.; Bagchi, B.; Zewail, A. H. *J. Phys. Chem. B* **2002**, *106*, 12376−12395.
(60) Kahlow, M. A.; Kang, T. J.; Barbara, P. F. *J. Chem. Phys.* **1988**, *88*, 2372−2378.
(61) Horng, M. L.; Gardecki, J. A.; Papazyan, A.; Maroncelli, M. *J. Phys. Chem.* **1995**, *99*, 17311−17337.
(62) Saha, S.; Mandal, P. K.; Samanta, A. *Phys. Chem. Chem. Phys.* **2004**, *6*, 3106−3110.
(63) Paul, A.; Samanta, A. *J. Phys. Chem. B* **2007**, *111*, 4724−4731.
(64) Hu, Z.; Margulis, C. J. *Acc. Chem. Res.* **2007**, *40*, 1097−1105.
(65) Castner, E. W., Jr.; Wishart, J. F.; Shirota, H. *Acc. Chem. Res.* **2007**, *40*, 1217−1227.
(66) Shirota, H.; Funston, A. M.; Wishart, J. F.; Castner, E. W., Jr. *J. Chem. Phys.* **2005**, *122*, 184512−184523.
(67) Arzhantsev, S.; Jin, H.; Baker, G. A.; Maroncelli, M. *J. Phys. Chem. B.* **2007**, *111*, 4978−4989.
(68) Jin, H.; Baker, G. A.; Arzhantsev, S.; Dong, J.; Maroncelli, M. *J. Phys. Chem. B* **2007**, *111*, 7291−7302.
(69) Chapman, C. F.; Maroncelli, M. *J. Phys. Chem.* **1991**, *95*, 9095−9114.
(70) Bart, E.; Meltsin, A.; Huppert, D. *J. Phys. Chem.* **1994**, *98*, 10819−10823.
(71) Bart, E.; Meltsin, A.; Huppert, D. *J. Phys. Chem.* **1994**, *98*, 3295−3299.
(72) Karmakar, R.; Samanta, A. *J. Phys. Chem. A* **2002**, *106*, 4447−4452.
(73) Karmakar, R.; Samanta, A. *J. Phys. Chem. A* **2002**, *106*, 6670−6675.
(74) Samanta, A. *J. Phys. Chem. Lett.* **2010**, *1*, 1557−1562.
(75) Headley, L. S.; Mukherjee, P.; Anderson, J. L.; Ding, R.; Halder, M.; Armstrong, D. W.; Song, X.; Petrich, J. W. *J. Phys. Chem. A* **2006**, *110*, 9549−9554.
(76) Song, X. *J. Chem. Phys.* **2009**, *131*, 044503−044510.
(77) Halder, M.; Headley, L. S.; Mukherjee, P.; Song, X.; Petrich, J. W. *J. Phys. Chem. A* **2006**, *110*, 8623−8626.
(78) Ito, N.; Arzhantsev, S.; Heitz, M.; Maroncelli, M. *J. Phys. Chem. B* **2004**, *108*, 5771−5777.
(79) Ingram, J. A.; Moog, R. S.; Ito, N.; Biswas, R.; Maroncelli, M. *J. Phys. Chem. B* **2003**, *107*, 5926−5932.
(80) Arzhantsev, S.; Ito, N.; Heitz, M.; Maroncelli, M. *Chem. Phys. Lett.* **2003**, *381*, 278−286.
(81) Shim, Y.; Choi, M. Y.; Kim, H. J. *J. Chem. Phys.* **2005**, *122*, 044511−044522.
(82) Shim, Y.; Jeong, D.; Manjari, S.; Choi, M. Y.; Kim, H. J. *Acc. Chem. Res.* **2007**, *40*, 1130−1137.
(83) Kobrak, M. N.; Znamenskiy, V. *Chem. Phys. Lett.* **2004**, *395*, 127−132.
(84) Kobrak, M. N. *J. Chem. Phys.* **2006**, *125*, 064502−064512.
(85) Bhargava, B. L.; Balasubramanian, S. *J. Chem. Phys.* **2005**, *123*, 144505−144512.
(86) Huang, X. H.; Margulis, C. J.; Li, Y. H.; Berne, B. J. *J. Am. Chem. Soc.* **2005**, *127*, 17842−17851.
(87) Kashyap, H. K.; Biswas, R. *J. Phys. Chem. B* **2008**, *112*, 12431−12438.
(88) Kashyap, H. K.; Biswas, R. *J. Phys. Chem. B* **2010**, *114*, 254−268.
(89) Rao, V. G.; Ghosh, S.; Ghatak, C.; Mandal, S.; Brahmachari, U.; Sarkar, N. *J. Phys. Chem. B* **2012**, *116*, 2850−2855.
(90) Hazra, P.; Sarkar, N. *Chem. Phys. Lett.* **2001**, *342*, 303−311.
(91) Hazra, P.; Chakrabarty, D.; Sarkar, N. *Langmuir* **2002**, *18*, 7872−7879.

(92) Pramanik, R.; Sarkar, S.; Ghatak, C.; Rao, V. G.; Sarkar, N. *J. Phys. Chem. B* **2011**, *115*, 2322−2330.
(93) Pramanik, R.; Ghatak, C.; Rao, V. G.; Sarkar, S.; Sarkar, N. *J. Phys. Chem. B* **2011**, *115*, 5971−5979.
(94) Moulik, S. P.; De, G. C.; Bhowmik, B. B.; Panda, A. K. *J. Phys. Chem. B* **1999**, *103*, 7122−7129.
(95) Adhikari, A.; Sahu, K.; Dey, S.; Ghosh, S.; Mandal, U.; Bhattacharyya, K. *J. Phys. Chem. B* **2007**, *111*, 12809−12816.
(96) Sasmal, D. K.; Mojumdar, S. S.; Adhikari, A.; Bhattacharyya, K. *J. Phys. Chem. B* **2010**, *114*, 4565−4571.
(97) Maroncelli, M.; Fleming, G. R. *J. Chem. Phys.* **1987**, *86*, 6221−6239.
(98) Fee, R. S.; Maroncelli, M. *Chem. Phys.* **1994**, *183*, 235−247.
(99) Bose, S.; Adhikary, R.; Mukherjee, P.; Song, X.; Petrich, J. W. *J. Phys. Chem. B* **2009**, *113*, 11061−11068.
(100) Headley, L. S.; Mukherjee, P.; Anderson, J. L.; Ding, R.; Halder, M.; Armstrong, D. W.; Song, X.; Petrich, J. W. *J. Phys. Chem. A* **2006**, *110*, 9549−9554.
(101) Mukherjee, P.; Crank, J. A.; Sharma, P. S.; Wijeratne, A. B.; Adhikary, R.; Bose, S.; Armstrong, D. W.; Petrich, J. W. *J. Phys. Chem. B* **2008**, *112*, 3390−3396.
(102) Balasubramanian, S.; Pal, S.; Bagchi, B. *Phys. Rev. Lett.* **2002**, *89*, 115505−115508.
(103) Chakraborty, A.; Seth, D.; Setua, P.; Sarkar, N. *J. Phys. Chem. B* **2006**, *110*, 5359−5366.
(104) Shirota, H.; Segawa, H. *Langmuir* **2004**, *20*, 329−335.
(105) Kashyap, H. K.; Biswas, R. *J. Phys. Chem. B* **2010**, *114*, 16811−16823.